

# Study on Porous Silk Fibroin Materials. II. Preparation and Characteristics of Spongy Porous Silk Fibroin Materials

MINGZHONG LI,<sup>1</sup> ZHENGYU WU,<sup>1</sup> CHANGSHENG ZHANG,<sup>1</sup> SHENZHOU LU,<sup>1</sup> HAOJING YAN,<sup>2</sup>  
DONG HUANG,<sup>1</sup> HUILAN YE<sup>1</sup>

<sup>1</sup> Material-Engineering Institute of Suzhou University, Ganjiang Eastern Road No. 178, Suzhou, China

<sup>2</sup> Dong Hua University, Yan'an Western Road No. 1882, Shanghai, China

Received 28 December 1999; accepted 7 June 2000

**ABSTRACT:** Porous silk fibroin materials, with average pore size 10 ~ 300  $\mu\text{m}$ , pore density 1 ~ 2000/ $\text{mm}^2$ , and porosity 35 ~ 70%, were prepared by freeze drying aqueous solution of silk fibroin obtained by dissolving silk fibroin in ternary solvent  $\text{CaCl}_2 \cdot \text{CH}_3\text{CH}_2\text{OH} \cdot \text{H}_2\text{O}$ . Pore size distribution of such materials mostly accorded with logarithmic normal distribution. It is possible to control the aforementioned structural parameters and the physical properties of moisture permeability, compressibility, strength, elongation, etc., by adjusting freezing temperature and concentration of silk fibroin solution. Above glass transition zone ( $-34 \sim -20^\circ\text{C}$ ) of silk fibroin, the freezing temperature has more significant effect on the structure and properties of porous silk fibroin materials. © 2001 John Wiley & Sons, Inc. *J Appl Polym Sci* 79: 2192–2199, 2001

**Key words:** silk fibroin; porous materials; freeze drying; pore characteristics; physical properties

## INTRODUCTION

High-purity silk fibroin fibers, as a kind of biopolymer, can be obtained easily from degummed silk. They can be dissolved in neutral salt solutions such as LiBr, LiSCN, and  $\text{CaCl}_2$ .<sup>1,2</sup> Their mixtures are dialyzed to get pure fibroin solution, which can be used to prepare silk fibroin membrane, gel, powder, etc. Silk fibroin is a kind of natural protein and is made up of eighteen kinds of amino acid such as Gly, Ala, Ser, etc. In addition to being used as surgical sutures and food additives, and used in the cosmetic industry,<sup>4–6</sup> silk fibroin has been studied in recent years as biomedical materials, such as

enzyme-immobilization materials, wound covering materials, artificial skins, soft contact lenses, anti-thromboplastic materials and dialysis membranes.<sup>7–12</sup> The results of various animal and clinical experiments with silk fibroin membrane used as wound-covering materials, indicated that silk fibroin has no toxicity or irritation, and have good biocompatibility.<sup>8</sup> Nowadays it is no longer a dream to prepare porous materials with silk fibroin and apply them in medical fields as matrices of cell culture, artificial skins, controlled drug delivery carriers, etc.

As regards the preparation methods of porous silk fibroin materials, one is by blending silk fibroin with polyethylene glycol (PEG), which will be dissolved away after membrane has formed<sup>13</sup>; the other is by freeze drying coagulated silk fibroin.<sup>14,15</sup> Freeze drying is a gentle drying means. It is favorable for alleviating the denaturation

Correspondence to: Mingzhong Li.

Contract grant sponsor: State Scientific and Technological Commission.

*Journal of Applied Polymer Science*, Vol. 79, 2192–2199 (2001)  
© 2001 John Wiley & Sons, Inc.

degree of protein, and to obtain porous materials with interconnecting pores. So it is a feasible way to prepare porous silk fibroin materials for medical use as matrices of cell culture, artificial skins, controlled drug delivery carriers, etc.

The previous article<sup>16</sup> reported the state change during heating of quick-frozen silk fibroin solution, which was prepared by dissolving silk fibroin in ternary solvent  $\text{CaCl}_2 \cdot \text{CH}_3\text{CH}_2\text{OH} \cdot \text{H}_2\text{O}$ , and the relationship between freeze drying conditions and the aggregated structure of silk fibroin. This article will report the relationship between freeze drying conditions, structural characteristics including pore size, pore density, and porosity, and physical properties such as moisture permeability, compressibility, strength, and elongation. It is aimed at seeking methods of preparing porous silk fibroin materials that can meet various using demands and have different structures and properties.

## MATERIALS AND METHODS

### Preparation of Silk Fibroin Solution

The *Bombyx mori* domestic silks were treated three times in 0.05 wt %  $\text{Na}_2\text{CO}_3$  solution at 98 ~ 100°C for 30 min respectively to remove sericin. After being air-dried, the refined silks were dissolved in ternary solvent  $\text{CaCl}_2 \cdot \text{CH}_3\text{CH}_2\text{OH} \cdot \text{H}_2\text{O}$  (mole ratio = 1:2:8) at  $78 \pm 2^\circ\text{C}$  through stirring. Then the mixed solution was dialyzed and filtered to get fibroin solution with concentration of about 2.7 wt %. Such solution was again stirred slowly at controlled temperature  $37 \pm 2^\circ\text{C}$  to make it evaporate and concentrate. Finally, silk fibroin solution with concentration of 7.4 ~ 16.7 wt % was prepared.

### Preparation of Porous Silk Fibroin Materials

After the addition of appropriate volume of crosslinking agent into aqueous solution of silk fibroin, the solution was poured into aluminum vessels with good heat transmissibility. Then they were frozen for 6 h at -80, -60, -40, -20, -16, -12, and  $-8^\circ\text{C}$ , respectively. Subsequently, it was vacuum dried by a VIRTIS GENESIS 25-LE Freeze dryer. After 24 ~ 28 h spongy and porous silk fibroin materials with no splits were prepared.

### Pore Characteristics Observing Methods of Porous Silk Fibroin Materials

The cross-sectional morphology of porous silk fibroin materials was observed by an Hitachi.S-570

Scanning Electron Microscope (SEM). The SEM photographs were scanned into computer in bmp form. The border of each pore in top layer was defined according to gradient method. Thus their pictures of the top layer of their cross sections were obtained. Each pore area  $x_1, x_2, \dots, x_i, \dots, x_n$ , and the area ( $S$ ) of porous silk fibroin material in statistic range, were calculated according to the limits of each pore in bmp and the number of picture points in the whole picture. And the pore radius ( $r_i$ ) of each pore, average pore radius ( $\bar{r}$ ), pore density ( $N$ ), and porosity ( $P$ ) were given by the following equations:

$$r_i = \left( \frac{x_i}{\pi} \right)^{1/2} \quad (1)$$

$$\bar{r} = \frac{\sum_{i=1}^n r_i}{n} \quad (2)$$

$$N = \frac{n}{S} \quad (3)$$

$$P = \frac{\sum_{i=1}^n x_i}{S} \quad (4)$$

### Physical Properties Measurement of Porous Silk Fibroin Materials

The moisture permeability of porous silk fibroin materials was measured according to the method of the water-vapor permeation cup.<sup>17</sup> A water-vapor permeation cup containing deionized water was sealed with samples and put upside-down in an environment ( $37 \pm 1^\circ\text{C}$ , 0 ~ 2% relative humidity). The weight of specimen combination was measured in every other hour. After 12 h the moisture permeation rate could be calculated from

$$\text{WVT} = \Delta m / S \Delta t \quad (5)$$

where WVT is the moisture permeation rate ( $\text{g}/\text{m}^2 \text{h}$ ),  $\Delta m$  is the weight difference of the same composite specimen between two times (g),  $S$  is the permeation area of specimen ( $\text{m}^2$ ), and  $\Delta t$  is the time interval between two weighings (h).

A compression tester division of instrumentation (KATO KES-FB3) measured compression behaviors including compression work, compression ratio, and compressive elasticity of the materials with the samples being cut into the shape of a square ( $3 \times 3$  cm).

A YGD21A Single Strand Strength Tester measured the stretchability with specimen width 10 mm and gripping length 40 mm.

The above measurements were all repeated at least three times with the same specimen, and the final data adopted were their average values.

## RESULTS AND DISCUSSION

### Effect of Freeze Drying Conditions on Structural Characteristics of the Pore

For vacuum-dried porous silk fibroin materials, when they were prepared at a freezing temperature of  $-80 \sim -20^\circ\text{C}$  by the method described above, they did not split and had a soft handle, and their appearance was white. The losing solution percentage was about 1%, when they were dissolved in warm water at  $37^\circ\text{C}$  by oscillation. However, when they were frozen above  $-20^\circ\text{C}$ , there was a slight yellow in the materials, the soft handle decreased slightly, and silk fibroin crystal flakes could be observed with the naked eye.

Figure 1 shows the SEM photographs of cross-sectional morphology of partial porous silk fibroin materials that were prepared at different freezing temperatures, and with identical concentration and vacuum-drying conditions. For those frozen below  $-20^\circ\text{C}$ , the pore shape took on irregular polygon and the pore arrangement had no certain direction. However, for those frozen above  $-20^\circ\text{C}$ , the pores took a leaf shape and the arrangement exhibited a relatively consistent direction. These phenomena resulted from the parallel arranged silk fibroin crystal flakes, which is attributed to the structural change of aggregating state of silk fibroin when freezing temperature was above its glass transition zone ( $-34 \sim -20^\circ\text{C}$ ).

Figure 2 shows the SEM photographs and the corresponding pore-size distribution of partial porous silk fibroin materials prepared with different concentrations and identical freezing temperature and vacuum-drying conditions. According to the statistic analysis, the pore area mostly accorded with logarithmic normal distribution. The density function of probability is as follows:

$$f(x) = \frac{1}{\sigma x (2\pi)^{1/2}} \exp\left[-\frac{(\ln x - \mu)^2}{2\sigma^2}\right]$$

where  $x$  is the pore area.

The average pore area is given as

$$E(X) = \exp(\mu + \sigma^2/2)$$

Pore area variance can be determined since

$$D(X) = \exp(2\mu + \sigma^2)[\exp(\sigma^2) - 1]$$

In the four cases of A, B, C, D in Figure 2 that were fitted with logarithmic normal distribution, the fitting coefficients are 0.9233, 0.8965, 0.9033, and 0.9771, respectively.

As shown in Figure 3 and Figure 4, with an increase of freezing temperature, pore diameter increased and pore density decreased. The change was slow in the range from  $-80$  to  $-20^\circ\text{C}$  and quick in the range from  $-20$  to  $-4^\circ\text{C}$ . When the porous silk fibroin materials prepared with silk fibroin solution of high concentration were frozen at the same temperature and dried at the same conditions, their pore diameter was small and the pore density was large.

After the ice in porous silk fibroin materials sublimated, many pores remained in them. In the course of freezing silk fibroin solution, when the temperature of water in the solution was below the freezing point and the solution was overfrozen, tiny ice nuclei formed due to heat exchange. As long as the degree of overdressing is high enough to keep the chemical potential of water in unstable phase higher than that of ice nuclei, the ice nuclei can grow into larger ice particles. Therefore the surrounding silk fibroin solution was condensed correspondingly, the distance between molecules in random coil structure shortened, and chain segments in different coils ran through each other and finally formed continuous silk fibroin solution phase. Because silk fibroin in glass state obstructed the motion of water molecules, the above process would last until its glass temperature. Following that, porous silk fibroin materials were obtained after the sublimation of ice diffusing in silk fibroin phase. From the afore-said forming process of pores, it is easy to see that the pore density in porous silk fibroin materials is in positive proportion to the number of ice nuclei per volume. That is, the more the ice nucleus forms during freezing, the larger is the pore den-

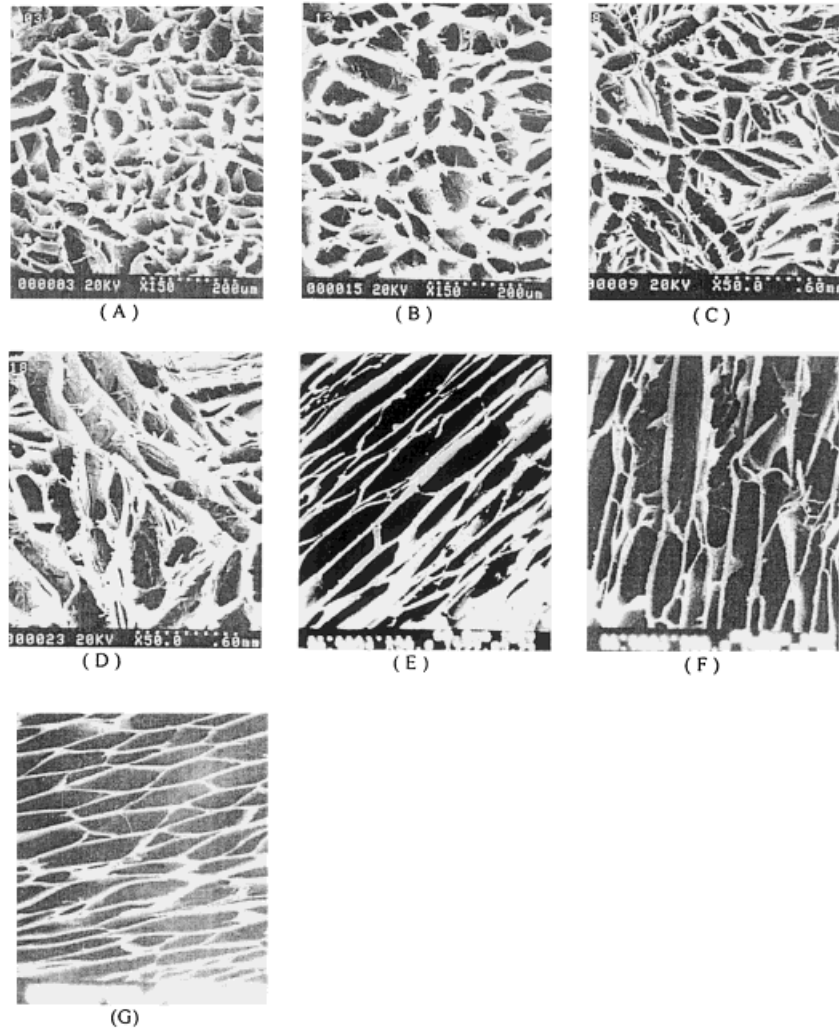


**Figure 1** Scanning electron micrographs of porous silk fibroin materials prepared under different freezing temperature (concentration of fibroin solution is 7.4 wt %): (A)  $-80^{\circ}\text{C}$  X150, (B)  $-60^{\circ}\text{C}$  X150, (C)  $-40^{\circ}\text{C}$  X50, (D)  $-20^{\circ}\text{C}$  X50, (E)  $-16^{\circ}\text{C}$  X50, (F)  $-12^{\circ}\text{C}$  X50, (G)  $-8^{\circ}\text{C}$  X20.

sity of vacuum-dried porous silk fibroin materials. The pore size is dependent on the size of ice particles; in more detail, the larger the ice particle formed during freezing is, the larger is the size of vacuum-dried porous silk fibroin materials.

During the freezing of pure water, the number ( $J$ ) of crystal nuclei per volume is mainly dependent on the temperature ( $T$ ) as described by the equation  $J = 10^{27} e^{-\Delta G/KT}$ ,<sup>18</sup> where  $\Delta G$  is critic free energy and  $K$  is Planck's constant. So the pore density of porous silk fibroin materials increases with the lowering of the freezing temperature. Apart from which it principally has relations with the concentration of silk fibroin solu-

tion, the structure of silk fibroin, and the combining manner of water and silk fibroin. The viscosity of silk fibroin solution with high concentration is large, which is unfavorable to the motion of water. So the probability of the formation of crystal nuclei is higher at the original position in water with the lowering of the temperature. And the pore density of porous silk fibroin materials increases with the increasing of the concentration of silk fibroin solution.

The size of ice particles forming during freezing silk fibroin solution is dependent on the growing velocity of ice crystals, growing time, growing history, etc. The lower is the freezing tempera-

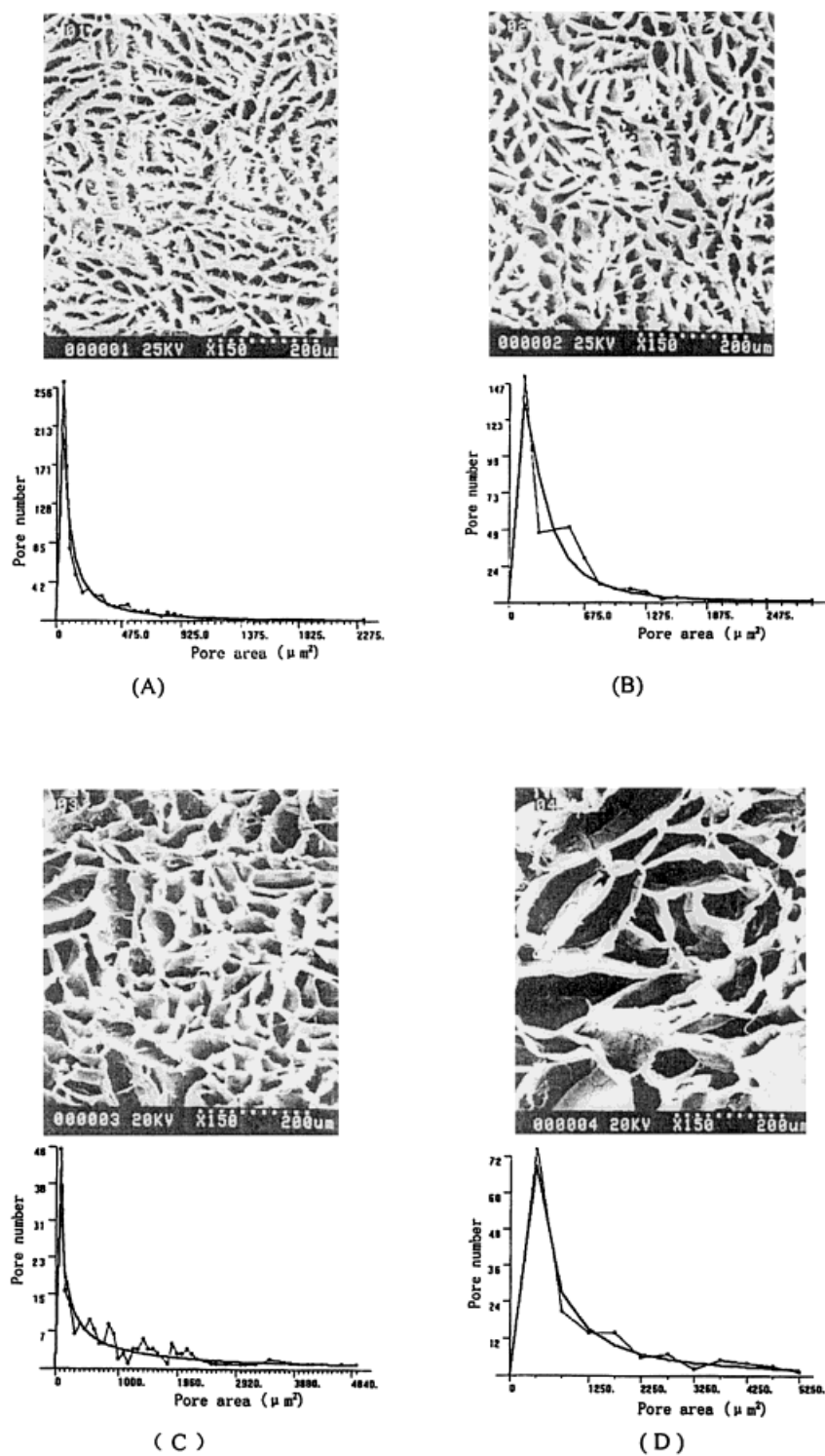


**Figure 2** Scanning electron micrographs and pore-area distribution of porous silk fibroin materials prepared under different fibroin concentration (freezing temperature  $-80^{\circ}\text{C}$ , X150; —○—: obtained through measurement; —: fitted with logarithmic normal distribution): (A) 16.7 wt %, (B) 12 wt %, (C) 7.4 wt %, and (D) 2.7 wt %.

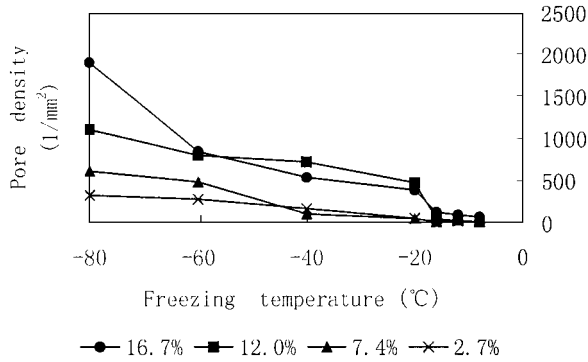


**Figure 3** Influence of freezing temperature and concentration of fibroin solution on pore density of freeze dried porous fibroin materials.

ture, the better is the heat transmissibility of the solution. If water molecules are subjected to small resistance when moving, ice crystals can grow quickly. Despite this, the temperature region within which ice crystals can grow is above the glass temperature of silk fibroin. Quick freezing often makes the temperature of silk fibroin exceed the region described above, which shortens the growing time of ice crystals and makes it difficult for them to form larger ice particles. So the pores in porous silk fibroin materials are small after they are vacuum dried and ice in them sublimates. However, the freezing temperature above glass transition zone ( $-34 \sim -20^{\circ}\text{C}$ ) favors the formation of larger ice particles, for it allows the water in an unstable phase more time to move toward the surface of ice particles. Silk fibroin solution with low concentration, in which the resistance to movement of water molecules is small

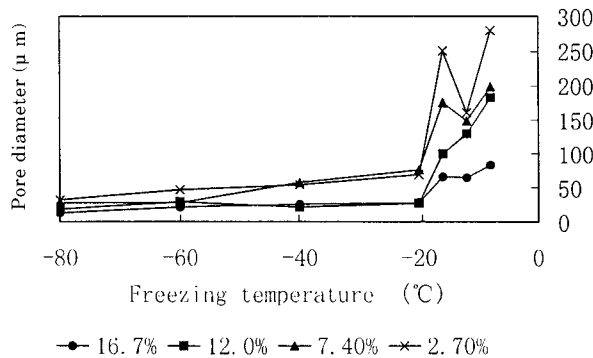


**Figure 4** Influence of freezing temperature and concentration of fibroin solution on pore diameter of freeze dried porous fibroin materials.

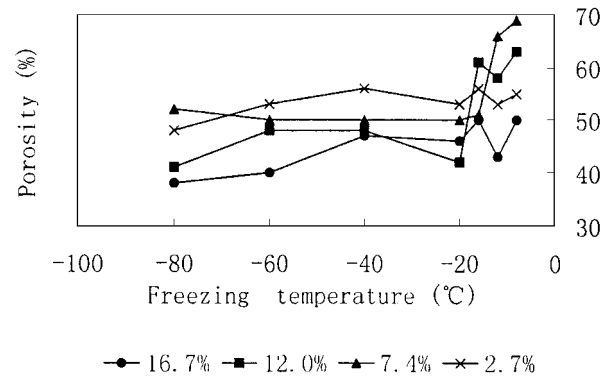


**Figure 5** Influence of freezing temperature and concentration of fibroin solution on porosity of freeze dried porous fibroin materials.

during freezing, is also favorable to the formation of larger ice particles. So pores in such porous silk fibroin materials are large.

The glass transition zone is an important region for the preparation of porous silk fibroin materials by freeze drying. The higher is freezing temperature when the temperature is above the zone, the longer is the time when ice particles can keep growing and the more effect on the pore size has freezing temperature. When it is below this region, the change of freezing temperature has less effect on the pore size.

The porosity of porous silk fibroin materials is dependent on the structure of aggregating state of silk fibroin as well as pore density and pore size. It can be seen in Figure 5 that porous silk fibroin materials with porosity 35 ~ 70% could be prepared by changing freeze drying conditions. Within the range from  $-80$  to  $-20^{\circ}\text{C}$ , the change of freezing temperature had no obvious effect on the porosity. However, when it was above  $-20^{\circ}\text{C}$ , the porosity increased, which may be due to the reason that freezing temperature above  $-20^{\circ}\text{C}$  is favorable to the crystallization of silk fibroin. When crystallization takes place partially in amorphous region, new voids are produced in the original amorphous regions.

Porous silk fibroin materials, with average pore size  $10 \sim 300 \mu\text{m}$ , pore density  $1 \sim 2000/\text{mm}^2$ , and porosity 35 ~ 70%, can be prepared according to the experiments in this article. It is possible to control the above characteristic parameters by adjusting freezing temperature, concentration of silk fibroin solution, and so on.

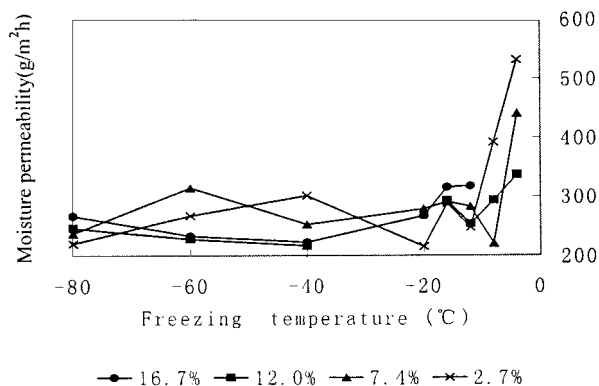


**Figure 6** Influence of freezing temperature and concentration of fibroin solution on moisture permeability of freeze dried porous fibroin materials.

### Effect of Freeze Drying Conditions on Physical Properties

On the condition that other conditions are identical, the moisture permeability of porous silk fibroin materials is decided by pore size and porosity, especially pore size having bigger influence. As shown in Figure 6, when temperature was above  $-20^{\circ}\text{C}$  the water-vapor permeation rate increased for the pore size becomes larger with the increasing of the freezing temperature. The change of freezing temperature within the range from  $-80$  to  $-20^{\circ}\text{C}$  has little effect on water-vapor permeation rate.

The compression work of porous silk fibroin materials can be used to characterize compressible degree of the materials. It is the work produced in the course of compressing the materials with pressure increased from 0.5 to 50  $\text{cN}/\text{cm}^2$ . Elastic recovery rate of compression work is the ratio of compression work to recovery work. It is the measure of compression elasticity of materials.

As shown in Figure 7 and Figure 8, when the freezing temperature was above  $-20^{\circ}\text{C}$  and kept increasing, the compression work increased and elastic recovery rate of compression work decreased. If the concentration of silk fibroin was high, the compression work of freeze dried materials was small and elastic recovery rate of compression work was big. This resulted from the joint influence of porosity of porous silk fibroin materials and other factors. That is, the materials of larger porosity have high compressible degree and poor compression elasticity. The change of freezing temperature within the range from  $-80$

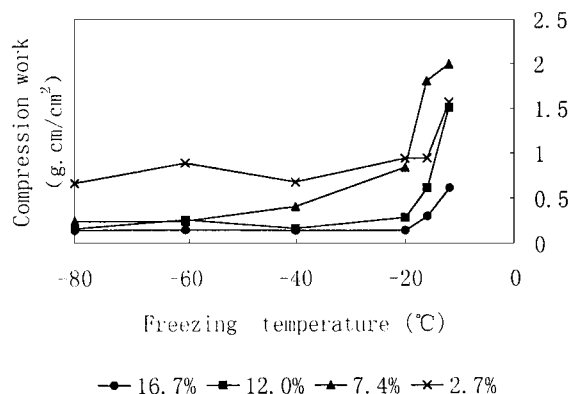


**Figure 7** Influence of freezing temperature and concentration of fibroin solution on compression work of freeze dried porous fibroin materials.

to  $-20^{\circ}\text{C}$  has no significant effect on the compressibility of porous silk fibroin materials.

The broken tensile strength and elongation of porous silk fibroin materials is related to porosity, pore size, structure of aggregating state, and so on. When the freezing temperature was in the range from  $-80$  to  $-20^{\circ}\text{C}$ , the structure of the aggregating state of silk fibroin in most parts was amorphous. With increasing temperature, the strength and elongation of silk fibroin materials decreased, as shown in Figure 9 and Figure 10, because pore size became bigger. When freezing temperature was above  $-20^{\circ}\text{C}$ , the strength and elongation increased to some extent with the increase of the crystallinity of silk fibroin in the aggregating state. When silk fibroin solution of high concentration was freeze dried, the strength and the elongation of the materials were high because the porosity was small.

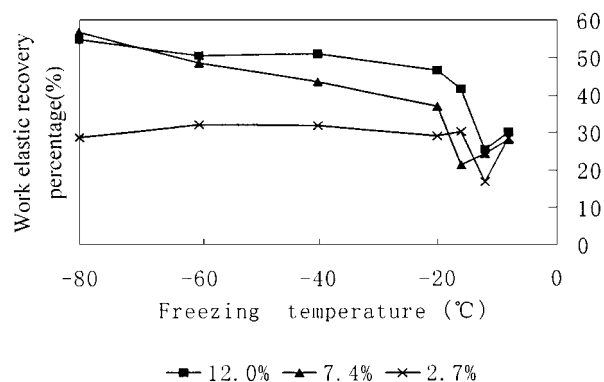


**Figure 8** Influence of freezing temperature and concentration of fibroin solution on Work elastic recovery percentage of freeze dried porous fibroin materials.

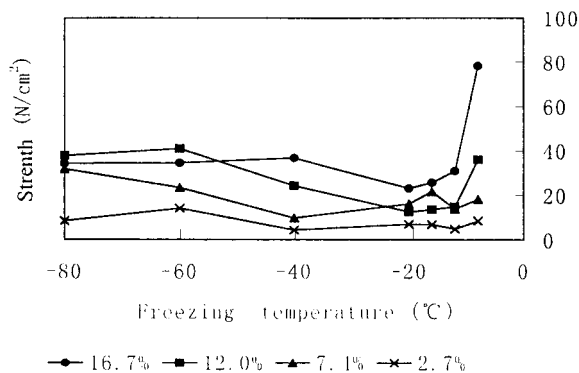


**Figure 9** Influence of freezing temperature and concentration of fibroin solution on tensile strength of freeze dried porous fibroin materials.

## CONCLUSIONS

Porous silk fibroin materials, which are of average pore size 10 ~ 300  $\mu\text{m}$ , pore density 1 ~ 2000/ $\text{mm}^2$ , and porosity 35 ~ 70% can be prepared by freeze drying the aqueous solution of silk fibroin, which was obtained by dissolving silk fibroin in ternary solvent  $\text{CaCl}_2 \cdot \text{CH}_3\text{CH}_2\text{OH} \cdot \text{H}_2\text{O}$ . Their pore-area distribution mostly accords with logarithmic normal distribution.

It is possible to control the above-mentioned structural parameters of porous silk fibroin materials and their physical properties such as mois-

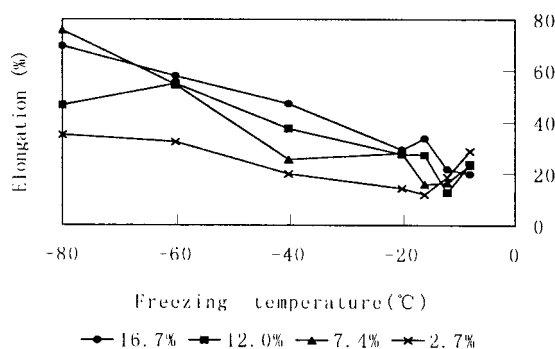


**Figure 10** Influence of freezing temperature and concentration of fibroin solution on elongation of freeze dried porous fibroin materials.

ture permeability, compressibility, strength, and elongation by adjusting the concentration of silk fibroin solution and freezing temperature.

The change of freezing temperature, which is above the glass transition zone ( $-34 \sim -20^\circ\text{C}$ ) of silk fibroin, affects the structure and characteristics of silk fibroin materials more significantly.

The authors are grateful to State Scientific and Technological Commission for financial support through the "863 plan" and Prof. Guoying Xu for her helpful discussions.

## REFERENCES

1. Ajisawa, A. *Nippon Sanshi Gakkaishi* 1969, 38, 340.
2. Ajisawa, A. *Nippon Sanshi Gakkaishi* 1969, 38, 365.
3. Minoura, N.; Tsukata, M.; Nagura, M. *Biomaterials* 1990, 11, 430.
4. Asakura, T. *Bioindustry* 1987, 4, 878.
5. Chen, K.; Iura, K.; Takano, R.; Hirabayashi, K. *J. Sericuet Sci Jpn* 1992, 62, 56.
6. Demura, M.; Xomura, T.; Asakura, T. *Sen-i Gakkaishi* 1990, 46, 391.
7. Tusbouchi, K. *PCT Int Appl WO* 9726927.
8. Wu, C.; Tian, B.; et al. *Properties and Applications of Wound Protective Membrane Made from Fibroin*; Third International Silk Conference, China, Suzhou, 1996.
9. Tamada, Y. *Jpn kokai Tokkyo koho*, JP09227402.
10. Minoura, N. In *Biomedical Applications of Polymeric Materials*; Tsuruta, T., et al., Eds.; CRC Press: Boca Raton, FL, 1993; p 128.
11. Li, M.; Saito, K.; Higa, M.; Tanioka, A. *Nippon Kaisui Gakkaishi* 1996, 50, 443.
12. Li, M.; et al. *J Textile Res* 1998, 19, 45.
13. Asakura, T.; Demura, M. *Sen-i Gakkaishi* 1988, 44, 535.
14. Tsukada, M.; Freddi, G.; Minoura, N.; Allara, G. *J Appl Polym Sci* 1994, 54, 507.
15. Sijia, M.; Toshinobu, N.; Akira, T.; Koji, A. *Sen-i Gakkaishi* 1998, 54, 85.
16. Li, M.; Lu, S.; Wu, Z.; et al. *Preceding article*.
17. State Standard of People's Republic of China, *Fabric Moisture Permeability Testing Method*, GB/T127049.
18. Maeno, N. *Refrigeration* 1998, 73, 11.